SCIENTIFIC REPORTS

OPEN

SUBJECT AREAS:
NONLINEAR OPTICS
QUANTUM PHYSICS
SOLID-STATE LASERS
OPTICAL MATERIALS AND STRUCTURES

Received
2 October 2012

Accepted
10 December 2012

Published
18 January 2013

Correspondence and requests for materials should be addressed to H.Z. (huaijinzhang@sdu.edu.cn)

# Generation of Crystal-Structure Transverse Patterns via a Self-Frequency-Doubling Laser

Haohai Yu[1,2], Huaijin Zhang[1], Yicheng Wang[1], Zhengping Wang[1], Jiyang Wang[1] & V. Petrov[2]

[1]State Key Laboratory of Crystal Materials and Institute of Crystal Materials, Shandong University, Jinan 250100, China, [2]Max-Born-Institute for Nonlinear Optics and Ultrafast Spectroscopy, 2A Max-Born-Strasse, 12489 Berlin, Germany.

**Two-dimensional (2D) visible crystal-structure patterns analogous to the quantum harmonic oscillator (QHO) have been experimentally observed in the near- and far-fields of a self-frequency-doubling (SFD) microchip laser. Different with the fundamental modes, the localization of the SFD light is changed with the propagation. Calculation based on Hermite-Gaussian (HG) functions and second harmonic generation theory reproduces well the patterns both in the near- and far-field which correspond to the intensity distribution in coordinate and momentum spaces, respectively. Considering the analogy of wave functions of the transverse HG mode and 2D harmonic oscillator, we propose that the simple monolithic SFD lasers can be used for developing of new materials and devices and testing 2D quantum mechanical theories.**

The observation of optical patterns is an excellent tool for studying the properties of quantum mechanics with or without chaos, quantized radiation fields, quantum optics, the concept of quantum-classical correspondence, *etc.*[1,2]. Recently, optical patterns possessing crystal- or quasicrystal-like structure have been widely investigated because they can be used to develop new materials and devices[3–5] and employed to implement different types of solitons[6–10], Anderson localization[11] and other quasiperiodic structures[12] by using the optical induction technique. Beside their implications in physics, they have attracted interest in other areas such as mathematics and art in both ancient and modern cultures[13,14]. Interference of multiple monochromatic point sources with specific symmetry[13,14] and superposition of multiple laser modes such as high-order Hermite-Gaussian (HG) and/or Laguerre-Gaussian (LG) modes[1,2] are two efficient methods for the generation of optical periodic and quasiperiodic structures.

It is well know that the paraxial wave equation for a laser propagating along z direction can be described by the Helmholtz equation: $\nabla^2 u + k^2 u = 0$ with $u = \psi(x,y)\exp(-ikz)$, here two dimensional (2D) $\psi(x,y)$ is a slowly varying complex function. The Helmholtz equation can also be expressed as: $\left(\nabla^2 - 2ik\frac{\partial}{\partial z}\right)\psi(x,y) = 0$. One can find that the Helmholtz equation shown above has a form similar to the time dependent 2D Schrödinger equation[15,16]. Therefore, their solutions are similar and optical laser patterns which express the solution of the Helmholtz equation have been applied to investigate 2D quantum information[17–19]. In this field, the eigenfunction of the 2D quantum harmonic oscillator (QHO) represents a fundamental issue[16] which can be used to illustrate the basic concepts and methods in quantum mechanics and has been applied in a variety of branches of modern physics, such as molecular spectroscopy, solid state physics, nuclear structure, quantum optics, and so forth. By simple transformation, the wave functions of the 2D QHOs can be described by the HG functions which are eigensolutions for the oscillating modes in a laser cavity. In the process of frequency doubling, two photons would "collide" with each other and propagate as one, and the resulted second-harmonic (SH) wave functions will be different even though they are dependent on the fundamental eigenfunctions. Therefore, the frequency doubling would induce the quantum state of the fundamental mode to become superposition of two macroscopically distinguishable states[20].

The self-frequency-doubling (SFD) process is a combination of laser emission and frequency doubling. The laser oscillating modes are determined by the cavity and the overlap with the pump beam. Through the nonlinear process, the oscillating photons would "recombine" and become visible to the naked eye. Therefore, SFD process should be practicable for studying the interaction of fundamental and SH modes, and the change of their quantum states. However, we are not aware of such investigations based on the SFD effect. In this work, we experimentally study the SH patterns of HG modes in a SFD microchip laser.

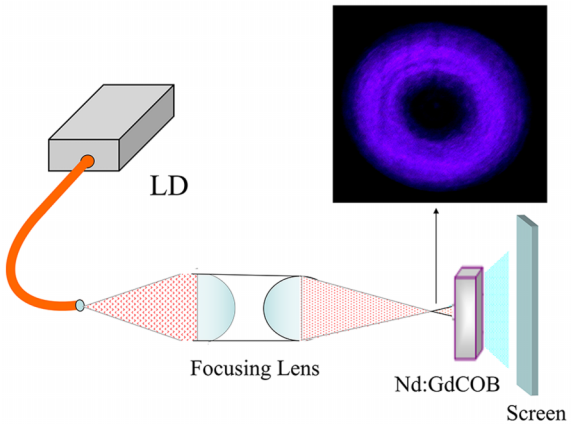


**Figure 1 | Experimental configuration for the SFD laser.** The pump beam from the fiber coupled LD with doughnut spatial profile (inset) is used to excite higher order transversal modes in the Nd:GdCOB SFD crystal. The visible output at the second-harmonic is directly projected onto a flat screen.

## Results

The SFD experiments was performed with a non-centrosymmetric crystal of Nd:GdCOB as the SFD crystal and a fiber coupled laser diode (LD) as the pump source whose output intensity profile from the fiber had a doughnut shape distribution. When the Fresnel number is small (<5), which means the length between the front face of the SFD crystal and the focal spot of the re-imaging unit is short, only the optical vortices were observed[21]. At that time, the doughnut-shape intensity profile dominated the fundamental laser and overlapped well with the LG modes. However, at a position of the SFD crystal with the front surface about 3-mm behind the focal spot, where the doughnut spatial profile of the pump beam is well pronounced, the threshold of the SFD laser operating in a high-order HG mode was 1.1 W. A typical SH pattern observed in the far-field is shown in Fig. 2a. It can be clearly seen that the far-field pattern exhibits a periodic lattice structure with the intensity localized at the center, which is different with the usual HG modes. Analyzing the symmetry of the pattern, it can be seen that each of the two orthogonal bright lines can be considered as a two-fold axis of symmetry. Rotation by 180° about any of the two-fold axes brings the pattern into coincidence with the original one. Therefore, the 2D crystal-like pattern possesses symmetry of 22. The near-field pattern was also observed and it is shown in Fig. 3a, representing the intensity distribution in coordinate space. It is seen that the near-field pattern is different and the intensity concentrated along a classically rectangular shaped trajectory with four peaks. The changing with propagation of SFD patterns is different with traditional HG modes whose appearances are unchanged[22].

By tuning the setup and maintaining the pump power of 1.1 W almost unchanged, the pattern can be changed which corresponds to different orders related to different mode spatial profiles which are better overlapped with different pump beam sizes. The near-field patterns are similar to the one shown in Fig. 3a. However, under the far-field observation, patterns for different orders exhibit different numbers of bright points. Typical experimentally observed far-field patterns for different orders are presented in Figs. 4a, and b. These patterns also possess crystal-like structure with 22 symmetry. It should be noted that, once the pattern with a certain order appeared, its structure was almost unchanged with time unless the setup was tuned. We believe that the stable structure may be generated by the good overlap between the pump and oscillating modes which only allows the optimal mode to oscillate near the threshold. As described in the **Methods** section, the output coupler of the present self-frequency-doubling microchip laser was high-transmission

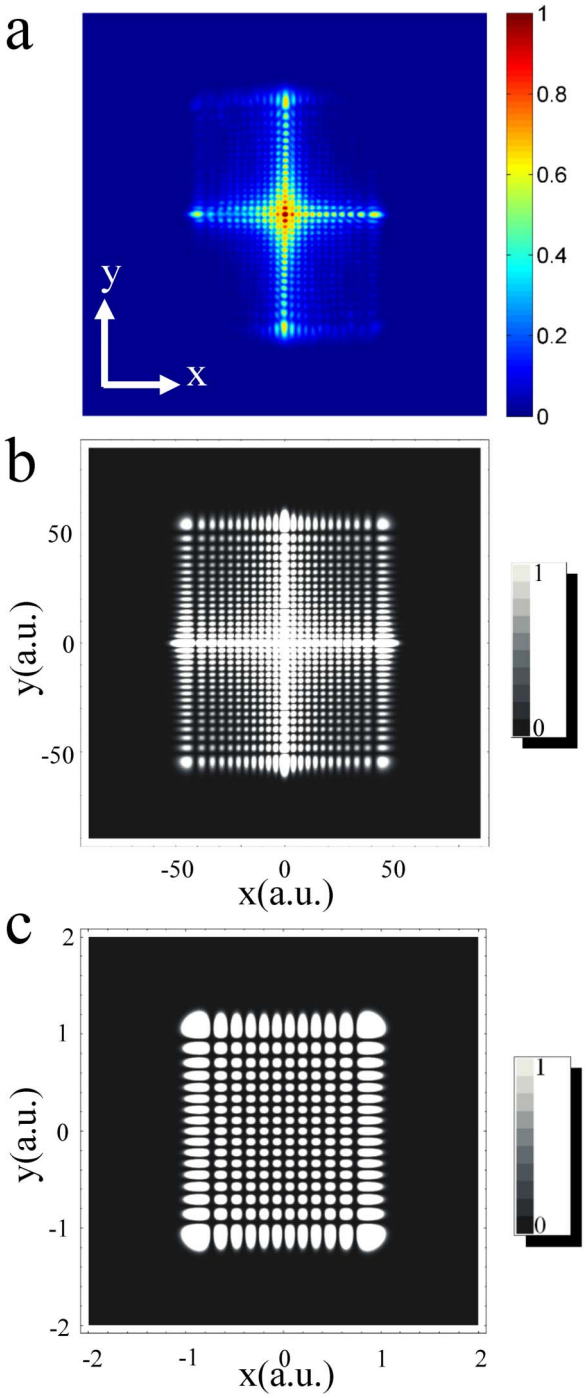


**Figure 2 | Far-field crystal-structure patterns at the second harmonic.** (a) Experimental observation of the far-field pattern at a pump power of about 1.1 W. (b) Theoretical calculation of the SH far field for a fundamental mode (11,16), and (c) HG eigenfunction of the same mode as in (b), calculated for the fundamental.

(HT, T>99%) in the 530-545 nm SH range, which means that the observed periodic visible modes did not oscillate in the cavity, their correlation coefficients should be zero and the gain distribution should be similar to the output pattern. The behavior of the present crystal-like structure patterns is different with the modes generated in the reported Talbot cavity[23,24].

The measured SFD laser wavelength was 545 nm, corresponding to the SH of the fundamental wavelength at 1090 nm. The SH beam was linearly polarized, corresponding to the "fast" eigenmode in the

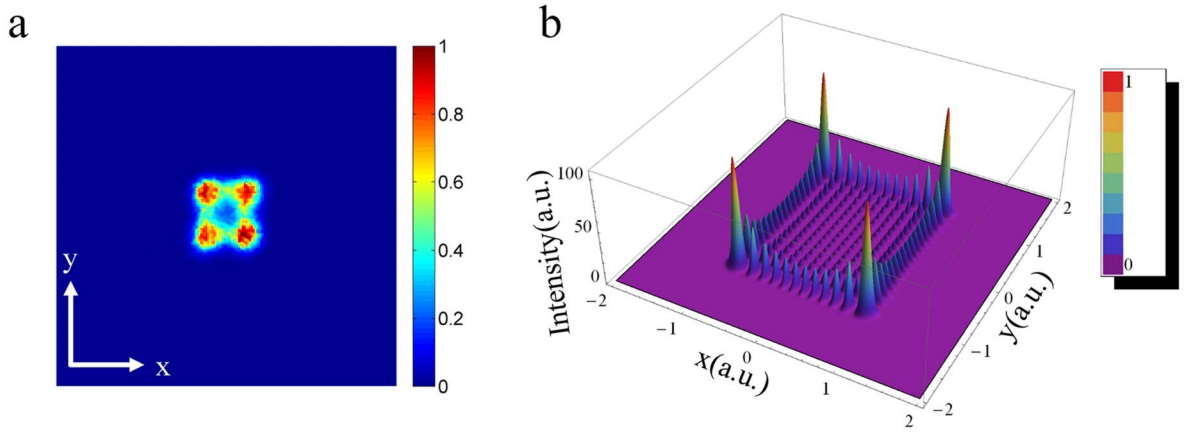


**Figure 3 | Near-field transverse patterns.** (a) Near-field diamond-shaped pattern experimental observed in the visible for conditions corresponding to Fig. 2a, and (b) Theoretical calculation for the relative intensity distribution of the near field second harmonic pattern based on the HG eigenfunction of the same fundamental mode (11, 16).

biaxial SFD crystal while the fundamental was with perpendicular polarization corresponding to the "slow" eigenmode. It should be noted that, when using a pump source whose spatial profile in the focal plane corresponds to a Gaussian-like distribution, we were unable to observe high-order HG SH modes. It can be believed that the doughnut distribution of the pump spot which determines the gain distribution in the laser medium is essential for excitation of higher order HG modes through selective spatial overlap. Compared with the generated high-order LG modes which is well described by the cylindrical coordinate[21], the symmetry of the emission cross-section of SFD crystal is also identified as an important factor for the generation of high-order HG modes. The symmetry of emission cross-section for Nd:GdCOB is $\infty mm$ with $\infty \| z$ axis which is well described by the Cavendish coordinate system[25] and agrees well with the symmetry of HG modes. Based on the analysis above, it can be obvious that, under small Fresnel number, the pump beam possesses

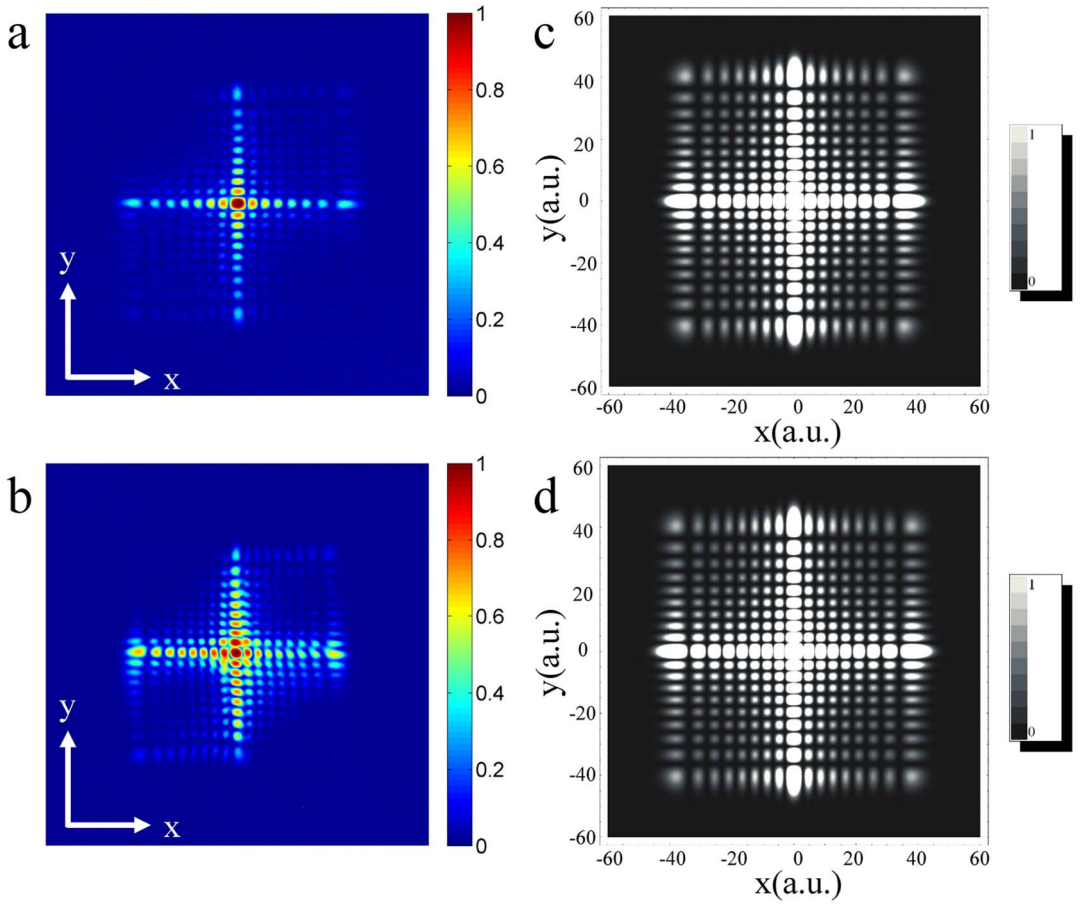


**Figure 4 | Far-field pattern of the SH with different (m, n) fundamental mode indices.** (a) Experimental observation and (c) theoretical calculation of the far-field SH pattern for fundamental mode (7, 9); (b) Experimental observation and (d) theoretical calculation of the far-field SH pattern for the fundamental mode (8, 9).

small size whose symmetry dominates the generated fundamental laser with LG modes; however, when the pump size becomes large enough, the symmetry of the emission cross-section induces the generation of high-order HG modes, since the gain distribution in the laser medium is determined by both of the pump intensity distribution and emission cross-section. Therefore, the generating mechanism for the crystal-structure patterns in SFD lasers is totally different with the previously investigated nonlinear optical system, such as photorefractive media[8] and vertical cavity surface emitting lasers[26] which are due to the nonlinearity of refractive index and reflection by their bounding, respectively. It should be noted that, under the observation, there was no typical vortex patterns accompanying or competing as shown in Fig. 2.

## Discussion

The eigenfunctions of the HG modes in a laser cavity are given by[22]

$$\Phi_{m,n}(x,y,z)=\frac{1}{\sqrt{2^{m+n-1}\pi m!n!}}\frac{1}{w(z)}H_m\left(\frac{\sqrt{2}x}{w(z)}\right)H_n\left(\frac{\sqrt{2}y}{w(z)}\right)e^{-\frac{(x^2+y^2)}{w(z)^2}}e^{i(m+n+1)\theta_G(z)}e^{-i\varsigma_{m,n,l}(x,y,z)} \quad (1)$$

with $w(z)=w_0\sqrt{1+(z/z_R)^2}$, $\theta_G(z)=\tan^{-1}(z/z_R)$ and $\varsigma_{m,n,l}(x,y,z)=(w_{m,n,l}z/c)\left[1+(x^2+y^2)/2\left(z^2+z_R^2\right)\right]$. Here, $w_0$ is the beam waist, $z_R$ is the Rayleigh range, $w_{\mathrm{m,n,l}}$ is the resonance frequency, m and n are the transverse mode indices, $l$ is the longitudinal mode index and $H_m$(x) is the m-th order Hermite polynomial. For a single HG mode, the phase does not affect the intensity distribution but it is essential for the Fourier transformation relating the near- and far-field distributions. In the near-field (z~0), the amplitude distribution is similar to that in the beam waist (z=0) and can be expressed in terms of HG functions:

$$E_{m,n}(x,y)=\frac{1}{\sqrt{2^{m+n-1}\pi m!n!}}\frac{1}{w_0}H_m\left(\frac{\sqrt{2}x}{w_0}\right)H_n\left(\frac{\sqrt{2}y}{w_0}\right)e^{-\frac{(x^2+y^2)}{w_0^2}} \quad (2)$$

As we know, the Hamiltonian for a 2D QHO can be shown as[19]:

$$H=i\hbar\frac{\partial}{\partial t}=\frac{p^2}{2\mu}+\frac{\mu\omega^2x^2}{2}+\frac{\mu\omega^2y^2}{2} \quad (3)$$

with the 2D momentum operator as:$p=-i\hbar\nabla$. The eigenfunctions for 2D QHO are given by:

$$\psi_{m,n}(x,y)=\left(\frac{\alpha}{\sqrt{\pi 2^{m+n}m!n!}}\right)H_m(\alpha x)H_n(\alpha y)e^{-\alpha^2(x^2+y^2)/2} \quad (4)$$

with $\alpha=\sqrt{\frac{\mu\omega}{\hbar}}$, where $\mu$ is the oscillator mass and ω is the angular frequency of the harmonic oscillator. Equating $\alpha=\frac{\sqrt{2}}{w_0}$, the HG transverse eigenmodes in the near field are equivalent to the eigenfunctions of the 2D QHO and can be used to simulate the mechanics of the 2D QHO. For the 2D QHO, the Eq. (4) represents the eigenfunction in the coordinate space. By Fourier transformation, the eigenfunction in the momentum space can be achieved from Eq. (4)[16]. Considering the Fourier transforming relationship between the transverse eigenmodes in the near and far fields based on the light propagating theory and the equivalence between the eigenfunctions of 2D QHO in the coordinate space shown in Eq. (4) and HG modes in the near field shown in Eq. (2), it can be reduced that the far-field HG transverse eigenmodes are analogous with the eigenfunctions of 2D QHO in the momentum space.

In SH generation, two photons collide with each other and combine into one with doubled photon energy and half wavelength. Based on the second-harmonic theory, the field amplitude for the fundamental $E_{m,n}$ and SH $E_{SH}$ can be expressed as:

$$\frac{\partial E_{m,n}}{\partial z}=\frac{if}{cn(f)}d_{eff}\mathrm{E}_{SH}\mathrm{E}^*_{m,n}\mathrm{e}^{i\Delta kz}$$
$$\frac{\partial E_{SH}}{\partial z}=\frac{if}{cn(2f)}d_{eff}\mathrm{E}^2_{m,n}\mathrm{e}^{-i\Delta kz} \quad (5)$$

with $\Delta k=k_2-2k_1$, where $d_{eff}$ is the efficient nonlinear coefficient, $n(f)$ and $n(2f)$ are the refractive indexes for the fundamental and SH wavelength, respectively, $f$ is the frequency of the fundamental light, $k_1$ and $k_2$ are the respective wave vectors of the fundamental and SH lights. For small signal approximation, the SH amplitude can be shown as:

$$E_{SH}(z)=\frac{if}{cn(2f)}d_{eff}E^2_{m,n}\int_0^z e^{-i\Delta kz}dz \quad (6)$$

Since the other parameters are constant for the phase matching $\Delta k=k_2-2k_1=0$, the resulted SH field amplitude of the SH is proportional to the square of the fundamental field distribution[27]:

$$E_{SH}(x,y)\propto E^2_{m,n}(x,y) \quad (7)$$

It should be noted that the large angular acceptance bandwidth and short length (6 mm) of the nonlinear crystal used[28] induce the ignorable effect generated by the divergence of high-order fundamental HG modes. If the SH field is decomposed to a linear combination of eigenfunctions of the 2D QHO or HG modes[29], the physics contained in the SH field may be more obvious. Since

$$H^2_m(x)H^2_n(y)=\sum_{p=0}^{m}\sum_{q=0}^{n}d^{m,n}_{2p,2q}H_{2p}(x)H_{2q}(y) \quad (8)$$

with

$$d^{m,n}_{2p,2q}=\frac{m!(2m-2p)!n!(2n-2q)!}{[(m-p)!]^2p!2^m[(n-q)!]^2q!2^n} \quad (9)$$

The SH field amplitude may be shown as:

$$E_{SH}\propto E^2_{m,n}(x,y)=\sum_{p=0}^{m}\sum_{q=0}^{n}c_{2p,2q}E_{2p,2q}(x,y) \quad (10)$$

here $c_{2p,2q}$ is the decomposed coefficient corresponding to the probability density of the 2D QHO in $\psi_{2p,2q}(x,y)$ state. Compared with Eq.s (2) and (10), it can be found that the SH light is composed by and localized on a superposed state of $E_{2p,2q}(x,y)$ or $\psi_{2p,2q}(x,y)$, with $p\le m$ and $q\le n$ which results in the eigenfunctions and localization of the SH light becoming different with the fundamental modes but possessing similar symmetry.

Using Eq.s (2) and (7) or (8), we calculated the intensity distribution in coordinate space for m=11, n=16, simplified as (11, 16), and the results is shown in Fig. 3b. It can be seen that light density is localized at four high intensity spots and decreases as x and y tend to 0, in good agreement with the experimental near-field pattern and similar with the fundamental HG mode whose structure would be unchanged with propagation. Based on an analysis using the Bohr correspondence principle and the classical areal velocity law[30], the probability density exhibits peaks at the points corresponding to the highest potential, just like a classical particle which would reside more time near the apogee of its motion.

As is well known, the far-field pattern corresponds to the momentum-space wave function which is the Fourier transformation of the coordinate-space wave function. The near-field pattern corresponds to the coordinate-space wave function. The far-field pattern can provide more useful information than the near-field one[31]. By Fourier transformation of Eq. (7), the far-field SH pattern can be calculated for (11, 16), as shown in Fig. 2b, and it resembles the experimentally obtained visible pattern. The theoretically calculated

far-field patterns for (7, 9), and (8, 9) are shown in Fig. 4c and d, respectively. From these figures, it can be clearly seen that the far-field pattern exhibits a periodic lattice structure with the same symmetry as the near-field pattern. For comparison, a calculated transverse mode distribution at the fundamental wavelength is also presented in Fig. 2c whose intensity distribution keeps unchanged and localized on four peaks similar with the observation of SFD in the near-field. It should be noted that the frequency-doubling resulted in intensity changed and localized at the center of the pattern, and the number of bright points along each transversal coordinate is larger but less than two times of the fundamental ones, although the symmetry is unchanged.

We proposed that, by mode conversion, angular momentum interactions between photons and nonlinear amplifying medium such as "angular momentum Raman-like scattering" may be realized and studied through the generated SFD pattern[32]. Because the HG modes can be employed to define an infinitely dimensional discrete Hilbert space[33] and SH generation is an important mechanism for realizing entangled states of lights[34] , this approach provides a route to investigate the entanglement involving many orthogonal quantum states. Similar to the nonlinear optical lattices which are dominated by the initial nonlinearity of the laser system and possess phase singularity and periodic structures[35,36], the present linear SFD patterns could also be used for the generation of periodic trapping fields due to the crystal-structure distribution of their intensity. Finally, the present method for direct generation of crystal structure patterns is based on a compact and simple design with easy control of the pattern and intensity distribution characteristics which could be applied for development of new materials and devices using the optical induction technology[3–5].

In conclusion, we observed 2D crystal-structure patterns with 22 symmetry analogous to a superposed state of the quantum harmonic oscillator in the near- and far-fields of the SH emission from a SFD microchip laser. Patterns of different orders are easy obtained by tuning. The laser modes based on the HG functions were calculated and compared with the experimental results. We believe that SFD visible lasers could become useful candidate besides two-wave mixing in photorefractive media and high-Fresnel laser cavities for testing quantum mechanical theories while the directly generated crystal-structure patterns could play an important role in developing new materials and devices.

## Methods

A non-centrosymmetric crystal of Nd:GdCOB grown by the Czochralski method with a Nd concentration of ~8 at.% was employed as an active element. This crystal is monoclinic biaxial and maximum effective nonlinearity for type-I SH generation with a fundamental wavelength of 1090 nm occurs in a phase-matched direction outside the principal planes; the 6-mm long sample was cut along this direction[37,38]. The 3 mm × 3 mm faces were polished and the front one was anti-reflection (AR) coated for 808 nm (pump) and high-reflection (HR, R>99.8%) coated for 1060–1091 nm (fundamental) and 532–545 nm (SH). The other face was HR coated for 808 nm and 1060–1091 nm, with high-transmission (HT, T>99%) in the 530–545 nm SH range. The two opposite faces of the crystal form a laser cavity which amplifies the light and generates the laser. The cavity ensures double pass pumping, the fundamental is not out-coupled, and the generated SH is completely out-coupled through the exit crystal face after one round trip. Thus, the self-frequency-doubling microchip laser consists of the pump source, cavity and Nd:GdCOB crystal. The experimental configuration is shown in Fig. 1. The pump source employed was a LD with a central wavelength around 808 nm coupled into a fiber with a core diameter of 200 μm and numerical aperture of 0.22. The output intensity profile from the fiber had a doughnut shape distribution. The pump light was focused onto the Nd:GdCOB crystal by a 1 : 1 re-imaging unit. To remove the heat generated, the Nd:GdCOB crystal was wrapped in indium foil and mounted in a water-cooled copper block. The laser spectrum was measured with an optical spectrum analyzer (AQ-6315, YOKOGAWA). The SH pattern was recorded with a 21 Megapixel digital camera (EOS 5D Mark II, Canon).


1. Chen, Y. F. & Lan, Y. P. Observation of laser transverse modes analogous to a SU(2) wave packet of a quantum harmonic oscillator. *Phys. Rev. A* **66**, 053812 (2002).
2. Stone, A. D. Nonlinear dynamics: Chaotic billiard lasers. *Nature* **465**, 696–697 (2010).
3. Mikhael, J., Roth, J., Helden, L. & Bechinger, C. Archimedean-like tiling on decagonal quasicrystalline surfaces. *Nature* **454**, 501–504 (2008).
4. Freedman, B., Bartal, G., Segev, M., Lifshitz, R., Christodoulides, D. N. & Fleischer, J. W. Wave and defect dynamics in nonlinear photonic quasicrystals. *Nature* **440**, 1166–1169 (2006).
5. Becker, J., Xavier, J., Boguslawski, M., Rose, P., Joseph, J. & Denz, C. Optically induced three-dimensional photonic lattices and quasi-crystallographic structures. *Proc. of SPIE* **7712**, 77123A (2010).
6. Fleischer, J. W., Carmon, T., Segev, M., Efremidis, N. K. & Christodoulides, D. N. Observation of Discrete Solitons in Optically Induced Real Time Waveguide Arrays. *Phys. Rev. Lett.* **90**, 023902 (2003).
7. Neshev, D. N., *et al.* Observation of discrete vortex solitons in optically induced photonic lattices. *Phys. Rev. Lett.* **92**, 123903 (2004).
8. Fleischer, J. W., Segev, M., Efremidis, N. K. & Christodoulides, D. N. Observation of two-dimensional discrete solitons in optically induced nonlinear photonic lattices. *Nature* **422**, 147–150 (2003).
9. Neshev, D., Ostrovskaya, E., Kivshar, Yu. S. & Krolikowski, W. Spatial solitons in optically induced gratings. *Opt. Lett.* **28**, 710–712 (2003).
10. Martin, H., Eugenieva, E. D., Chen, Z. G. & Christodoulides, D. N. Discrete solitons and soliton-induced dislocations in partially coherent photonic lattices. *Phys. Rev. Lett.* **92**, 123902 (2004).
11. Schwartz, T., Baral, G., Fishman, S. & Segev, M. Transport and Anderson localization in disordered two-dimensional photonic lattices. *Nature* **446**, 52–55 (2007).
12. Wang, X., Ng, C. Y., Tam, W. Y., Chan, C. T. & Sheng, P. Large-area two-dimensional mesoscopic quasi-crystals. *Adv. Mater.* **15**, 1526–1528 (2003).
13. Lu, P. J. & Steinhardt, P. J. Further notes on quasi-crystal tilings. *Science* **316**, 981–982 (2007).
14. Chen, Y. F., Liang, H. C., Lin, Y. C., Tzeng, Y. S., Su, K. W. & Huang, K. F. Generation of optical crystals and quasicrystal beams: Kaleidoscopic patterns and phase singularity. *Phys. Rev. A* **83**, 053813 (2011).
15. Kogelnik, H. & Li T. Laser beams and resonators. *Appl. Opt.* **5**, 1550–1567 (1966).
16. Sakurai, J. J. *Modern Quantum Mechanics,* Wesley Publishing Company, Inc. (1994).
17. Gräf, H.-D. *et al.* Distribution of eigenmodes in a superconducting stadium billiard with chaotic dynamics. *Phys. Rev. Lett.* **69**, 1296–1299 (1992).
18. Stöckmann, H. J. *Quantum Chaos—An Introduction,* Cambridge University Press, Cambridge, (1999).
19. Nöckel, J. U. & Stone, D. Nonlinear dynamics: Chaotic billiard lasers. *Nature* **385**, 45-47 (1997).
20. Bhawalkar, D. D., Colles, M. J. & Smith, R. C. Mode conversion in optical second harmonic generation: Theory and experiment. *Opt-Electron.* **2**, 90 (1970).
21. Yu, H. H., *et al.* Experimental observation of optical vortex in self-frequency-doubling generation. *Appl. Phys. Lett.* **99**, 241102 (2011).
22. Nienhuis, G. & Allen L. Paraxial wave optics and harmonic oscillators. *Phys. Rev. A* **48**, 656–665 (1993).
23. Okulov, A. Yu. Scaling of diode-array-pumped solid-state lasers via self-imaging. *Opt. Commun.* **99**, 350–354 (1993).
24. Okulov, A. Yu. The effect of roughness of optical elements on the transverse structure of a light field in a nonlinear Talbot cavity. *J. Mod. Opt.* **38** 1887–1890 (1991).
25. Shao, Z. S., Lu, J. H., Wang, Z. P., Wang, J. Y. & Jiang, M. H. Anisotropic properties of Nd:ReCOB (Re=Y,Gd):a low symmetry self-frequency doubling crystal. *Prog. Cryst. Growth & Character. Mater.* **40**, 63–73 (2000).
26. Huang, K. F., Chen, Y. F., Lai, H. C. & Lan, Y. P. Observation of the wave function of a quantum billiard from the transverse patterns of vertical cavity surface emitting lasers. *Phys. Rev. Lett.* **25**, 224102(2002).
27. Dholakia, K., Simpson, N. B., Padgett, M. J. & Allen, L. Second-harmonic generation and the orbital angular momentum of light. *Phys. Rev. A* **54**, 3742–3745 (1996).
28. Yoshimura, M., Furuya, H., Kobayashi, T., Murase, K., Mori, Y. & Sasaki, T. Noncritically phase-matched frequency conversion in $Gd_xY_{1-x}Ca_4O(BO_3)_3$ crystal. *Opt. Lett.* **24**,193–195(1999).
29. Nikitint, S. P. & Masalov, A. V. Quantum state evolution of the fundamental mode in the process of second-harmonic generation. *Quantum Opt.* **3**, 105–113 (1991).
30. Pollet, J., Méplan, O. & Gignoux, C. Elliptic eigenstates for the quantum harmonic oscillator. *J. Phys. A: Math. Gen.* **28**, 7287–7297 (1995).
31. Huang, K. F., Chen, Y. F., Lai, H. C. & Lan, Y. P. Observation of the wave function of a quantum billiard from the transverse patterns of vertical cavity surface emitting lasers. *Phys. Rev. Lett.* **89**, 224102 (2002).
32. Arnaut, H. H. & Barbosa, G. A. Orbital and intrinsic angular momentum of single photons and entangled pairs of photons generated by parametric down-conversion. *Phys. Rev. Lett.* **85**, 286–289 (2000).
33. Mair, A., Vaziri, A., Weihs, G. & Zeilinger, A. Entanglement of the orbital angular momentum states of photons. *Nature* **412**, 313–316 (2001).
34. Grosse, N. B., Bowen, W. P., McKenzie, K. & Lam, P. K. Harmonic Entanglement with Second-Order Nonlinearity. *Phys. Rev.Lett.* **96**, 063601 (2006).
35. Okulov, A. Yu. 3D-vortex labyrinths in the near field of solid-state microchip laser. *J. Mod. Opt.* **55,** 241–259 (2008).
36. Chen, Y. F. & Lan, Y. P. Formation of optical vortex lattices in solid-state microchip lasers: spontaneous transverse mode locking. *Phys. Rev. A* **64**, 063807 (2001).

37. Wang, J. Y., *et al.* Watt-level self-frequency-doubling Nd:GdCOB lasers. *Opt. Express* 18, 11058–11063 (2010).
38. Lucas-Leclin, G., *et al.* Determination of the nonlinear optical coefficients of $YCa_4O(BO_3)_3$ crystal. *J. Opt. Soc. Am. B* **17**, 1526–1530 (2000).

## Acknowledgement

The authors wish to thank Prof. R.I. Boughton, Department of Physics and Astronomy of Bowling Green State University, for useful discussions on physics and linguistic advice. H. H. Yu wishes to thank the support by Alexander von Humboldt foundation. This work is supported by the National Natural Science Foundation of China (No. 51025210 and 51102156) and the National High Technology Research and Development Program ("863"Program) of China (No.2009AA03Z436), Grant for State Key Program of China (2010CB630702).

## Author contributions

H.H.Y. and H.J.Z. contributed equally to this work, conceived the experiments, performed the experiments, collected and analyzed the data, and wrote the paper; Y.C.W. and J.Y.W. grew the crystal; Z.P.W. and V.P. helped with the data analysis, theoretical calculation and paper writing.

## Additional information

**Competing financial interests:** The authors declare no competing financial interests.



**How to cite this article:** Yu, H. *et al.* Generation of Crystal-Structure Transverse Patterns via a Self-Frequency-Doubling Laser. *Sci. Rep.* **3**, 1085; DOI:10.1038/srep01085 (2013).